Inorganic Chemistry

Article

pubs.acs.org/IC

Local Supersaturation Dictated Branching and Faceting of Submicrometer PbS Particles with Cubic Growth Habit

Mingzhu Liu,[†,‡,∥] Mei Leng,[⊥,†,∥] Dan Liu,[†] Fanglin Chen,*[,§] Chengyu Li,[†] and Cheng Wang*[,†]

[†]State Key Laboratory of Rare Earth Resource Utilization, Changchun Institute of Applied Chemistry, Chinese Academy of Sciences, Jilin, 130022, P. R. China

[‡]School of Chemistry and Materials Science, Huaibei Normal University, Huaibei, 235000, P. R. China

[§]Department of Mechanical Engineering, University of South Carolina, 300 Main Street, Columbia, South Carolina 29208, United States

Supporting Information

ABSTRACT: Hierarchical cubelike submicrometer PbS particles consisting of truncated octahedrons, cuboctahedrons, and cubes were prepared in ethylene glycol solution under favorable high mole ratio of thiourea (Tu) to $Pb(AC)_2$ ($R_{S/Pb}$) via a pumping process. A qualitative analysis based on the classical nucleation theory coupled with the crystal growth theory is employed to interpret the observed experimental phenomena. By varying the concentration of reactants, $R_{S/Pb}$, and reaction temperature, it is possible to tune the local supersaturation degree (LSD), which is determined by the number of nuclei and overall growth unit (or concentration), surrounding each growing particle that dictates the branching and faceting of PbS particle. Relatively high LSD that is required for branching growth could be achieved at lower concentration of Tu and reaction temperature. Increasing the concentration of Tu and reaction temperature resulted in less LSD and yielded cubic PbS particles.

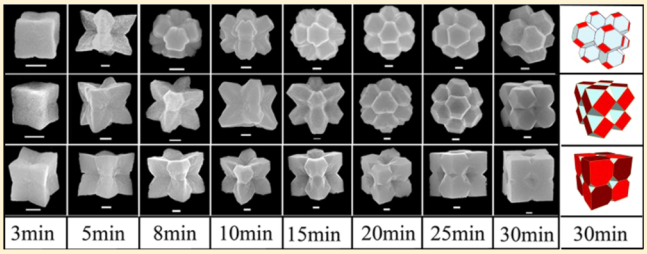

INTRODUCTION

Numerous findings showed that many physical properties and practical applications of nano- and submicrometer scaled materials relied on their particle size, monodispersity, and shapes.[1] Polyhedral nano- and submicro structures were usually highly symmetric particles with well-defined shapes. The synthesis of polyhedral noble metal nano- particles via solution-based processes caught the foremost attention and has achieved substantial success due to their fascinating optical properties and highly catalytic activities.[2,3] The solution-based approach has been then extended to the synthesis of binary or tertiary polyhedral compounds such as Cu_2O[4] and $CuInS_2$,[5] with their dimensional sizes below micrometer scale.

In solution-based methods, monodispersed colloids could be arrested with the guideline of Lamer model.[6] The vapor−liquid−solid (VLS)[7,8] and dislocation-driven[9] mechanisms have been deployed for the growth of one-dimensional nanowires or nanotubes prepared from chemical/physical vapor deposition or solution processes. For polyhedral nano- and microstructures synthesized in solution media, their formations have been generally ascribed to the anisotropic growth of different crystalline planes with various surface energies.[1,10] The resultant morphologies usually follow the Gibbs−Wulff theorem.[11,12]

Besides regular polyhedral structures, branched and dendritic materials have been also produced.[13,14] To understand the growth habit and branching of particles with sizes in the micrometer range, Siegried and Choi systematically studied the branching and faceting of Cu_2O via electro-crystallization processes.[15,16] They found that both anions such as dodecyl sulfate, Cl^-, NO_3^- or SO_4^{2-} and cation-like NH_4^+ could be used to control the growth habits of Cu_2O.[17] The degrees of branching and architectures of microsized Cu_2O crystals could be regulated by controlling the deposition potential/current or changing the growth media.[16] They were inclined to ascribe their observations to the deployed electrochemical parameters.

Here, we report the synthesis of branched and faceted submicrometer PbS particles with cubic growth habit also in solution processes. As a traditional semiconductor material with a very small direct band gap of 0.41 eV,[18] PbS has a stable rock-salt structure and becomes more important due to its promising properties and applications.[19−21] A lot of efforts have been made to synthesize PbS with diverse morphologies and sizes varied from nano- to micrometer scale via either solution or vapor-phase approaches.[22−26] In this work, the synthetic protocol was modified from our previous method[27] through decreasing the concentrations of precursors and reaction temperature. Three kinds of hierarchical cubelike submicrometer PbS particles consisting of truncated octahedrons, cuboctahedrons, and cubes could be obtained. A qualitative analysis based on the classical nucleation theory coupled with

Received: June 10, 2014
Published: October 23, 2014

   dx.doi.org/10.1021/ic501368y | Inorg. Chem. 2014, 53, 11484−11491

the crystal growth theory revealed that the observed morphological evolutions of these three typical products were mainly dictated by the local supersaturation degree (LSD) surrounding each individual particle, which dominates the growth mechanism during the growth process of the products. It is concluded that at higher LSD and lower $R_{S/Pb}$, the kinetics-controlled growth promotes branching growth and the dominance of the {111} facets, whereas at less LSD and high $R_{S/Pb}$, the more stable {100} facets are favored.

EXPERIMENTAL SECTION

Chemicals. All chemicals were commercially available and used as received without further purification. Lead(II) acetate ($Pb(Ac)_2 \cdot 3H_2O$), thiourea (Tu), ethylene glycol (EG), and poly(vinylpyrrolidone) (PVP-K30, 6.0×10^{-3} mol in terms of repeating unit, molecular weight ≈ 50 000) were obtained from Shanghai Lite Chemical Technology Co., Ltd.

Synthesis of Submicrometer PbS Particles. Typically, a mixture containing 0.66 g of PVP-K30, a certain amount of thiourea (Tu), and 8.0 mL of EG was added into a 50.0 mL three-neck flask and heated to 100 °C under magnetic stirring until a clear solution was formed. To this mixture was added 76 mg of $Pb(Ac)_2 \cdot 3H_2O$ (2.0×10^{-4} mol) dissolved in 1.0 mL using a peristaltic pump (HL-2D, Qingpu Huxi Instrument Factory, Shanghai) at a rate of 10.0 mL·h^{-1}. The reaction was kept at the same temperature for desired duration.

To study the time-dependent evolutions of the product, the reactions were interrupted by stopping the introduction of $Pb(Ac)_2 \cdot 3H_2O$ at 3.0 or 5.0 min before the pumping was finished (6.0 min), and then the flask was removed from the heating mantle; this was followed with pouring 20 mL of double distilled (DD) water into the flask. For the other cases, 1.0 mL aliquots of the reaction solutions were taken from the reaction systems at different intervals after finishing pumping the solution of $Pb(Ac)_2 \cdot 3H_2O$ and were injected into a vial containing 5.0 mL of DDI water. The products were collected after centrifugation, washed by ethanol and water three times, and dried at 60 °C.

Characterization. Powder X-ray diffraction (XRD) measurements were performed on a Bruker D8 Focus diffractometer with Cu Kα radiation and a Lynx Eye detector at a scanning rate of 15.0°/min. Field emission scanning electron microscopy (FESEM) images were taken using Hitachi S-4800 scanning electron microscope operated at an acceleration voltage of 10.0 kV. Transmission electron microscopy (TEM) images were taken using an FEI Tecnai F20 transmission electron microscopy operated at an accelerating voltage of 200 kV.

RESULTS

The synthetic protocols were adopted from our previous work[27] with some modifications. Both the concentrations of reactants and reaction temperature were reduced to allow slower reactions. The growth of submicrometer PbS particles was synergistically controlled by many deployed synthetic conditions.

The effect of the amount of Tu added on the morphology. The preparation of submicrometer PbS particles were fulfilled by pumping the solution containing 76 mg of $Pb(Ac)_2 \cdot 3H_2O$ into the flask, in which 0.66 g of PVP-K30 and different amounts of Tu were predissolved in 8.0 mL of EG. The overall concentration of $Pb(Ac)_2 \cdot 3H_2O$ in this process is about one-fifth of that used previously. More importantly, the reaction temperature was lowered from 160 to 100 °C. With these two modifications, the reaction became much slower, and the reaction time was accordingly prolonged to complete the reaction. Since the addition speed of $Pb(Ac)_2 \cdot 3H_2O$ solution was quite low and the tube length in peristaltic pump is about 1.0 m, it took a while for the $Pb(Ac)_2 \cdot 3H_2O$ solution to be transferred from its container to the flask. The reaction time throughout this manuscript was counted once the first droplet of $Pb(Ac)_2 \cdot 3H_2O$ solution was added to the flask.

Figure 1a–e shows the hierarchical structures of the obtained products after reaction at 100 °C for 30 min by adding 57, 68, 76, 100, or 200 mg of Tu into the flask. Their average particle sizes were in the range of 500 to 700 nm. When 57 mg of Tu was used, the resultant product was dominated by hierarchical particles consisting of eight truncated suboctahedrons (Figure 1a). Along with this, some particles were also presented and appeared to be truncated octahedrons with their six {100} faces or/and 12 edges unfilled. The hierarchical structure of the dominant product could be depicted more clearly from its simulated structure shown in Figure 1f. Each truncated suboctahedron was connected with its three neighboring truncated suboctahedrons via sharing three of the six {100} faces. The coexisted truncated octahedral particles with unfilled vertices and edges could be viewed as a result of partially filling the gaps among eight small suboctahedrons.

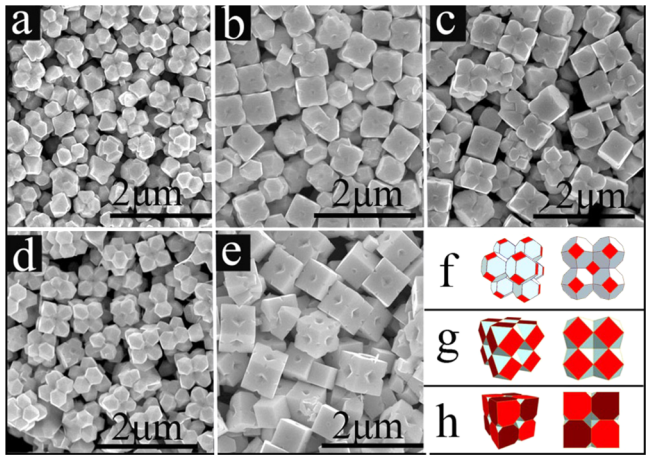

Figure 1. FESEM images of branched cube-like PbS submicrometer particles consisting of truncated octahedrons (a), cuboctahedrons (b, c, and d), and cubes (e) obtained at 100 °C after 30 min of reaction using 57 mg (a), 68 mg (b), 76 mg (c), 100 mg (d), and 200 mg (e) of Tu. Simulated structures of the three typical morphologies are given in (f, g, and h). In all cases, the LSDs are kept at relatively high degree to maintain their branching growth, and the morphologies of the branched subunits are determined by the $R_{S/Pb}$ ratio, similar to our previous observation,[26] in which we found that octahedral, truncated octahedral, and cubelike particles were prepared with increasing $R_{S/Pb}$ value.

Increasing the weight of Tu to 68 mg, the product became cubelike particles with unfilled face-center, broken edges, and truncated vertices (Figure 1b). Further increasing the amount of Tu to 76 mg, some particles had similar morphology to those in Figure 1b, while others were cubelike, and hierarchical particles consisting of eight subcuboctahedrons (Figure 1c). Actually, the product presented in Figure 1b could be also viewed as a hierarchical structure, and its subunits were similar to those in Figure 1c except the truncation degree of the vertices of the subcuboctahedrons, which correspond to the {111} faces. The former one had a slight truncation degree, while the latter one was bigger. Each subcuboctahedron fused with its three neighborings via three of the six {100} faces, similar to the suboctahedrons in Figure 1a. When 100 mg of Tu was used, the cubelike particles in the product had more obvious hierarchical structure with more severe truncation degree for the eight {111} faces of each cuboctahedral subunit

dx.doi.org/10.1021/ic501368y | Inorg. Chem. 2014, 53, 11484–11491

(Figure 1d). A simulated structure with half truncation of {111} faces is illustrated in Figure 1g.

Further increasing the amount of Tu to 200 mg (Figure 1e), the product had unfilled face-centers and broken edges and presented inconspicuous hierarchical structure, similar to that shown in Figure 1b except the morphology of the subunits. Eight subunits in Figure 1e were nearly fully developed cubes with seven of their eight vertices slightly truncated, differing from subcuboctahedron (Figure 1b) in which all eight corners are truncated. The simulated structure of product in Figure 1e is presented in Figure 1h.

Time-Dependent Morphological Evolutions. To get insights into the growth mechanisms of the three typical morphologies (i.e., the eight small subunits are truncated octahedrons, cuboctahedrons, and cubes), time-dependent products from different reaction intervals were harvested to reveal their morphological evolutions. For the three products prepared at 68, 76, and 100 mg, only the reaction using 76 mg of Tu was chosen since they are all comprised of small subcuboctahedrons and bear similar evolutions. All XRD patterns (Supporting Information, Figure S1) of the three typical products shown in Figure 1a,c,e obtained at different stages could be indexed to phase-pure cubic PbS (JCPDS Card No. 05−0592). The products are well-crystallized. It should be mentioned here that the intensities of the diffraction peaks are arbitrary. The intensity variation among different peaks does not mean that their crystallinities differ from each other, especially for the products at early stages, for example, 3 and 5 min, as their amounts for XRD characterization were different. FESEM images shown in Figure 2 depict the growth histories of these three kinds of particles. The panoramic images of the products corresponding to those shown here are provided in Supporting Information, Figures S2−S4. Initially, at the reaction time of 3 min, all products were small and nearly cubelike particles with distorted edges when viewed along ⟨100⟩ directions. Tilted from this direction, it can be seen that the faces were concaved. The distortion degree increases along with the increase of the amount of Tu as shown in the 3 min column, suggesting that branching growth tends to occur when higher concentration of Tu was used in the flask. After pumping $Pb(Ac)_2{\cdot}3H_2O$ solution for 5 min, the eight corners of all three kinds of particles tend to protrude further, and the branching degree became more prominent.

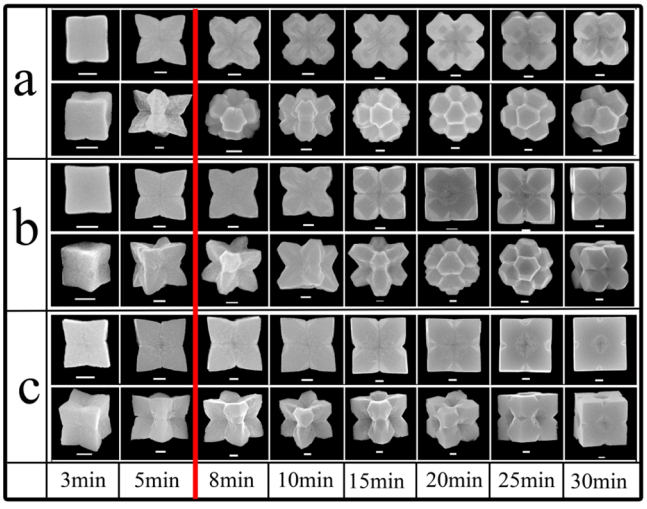

Figure 2. Time-dependent FESEM images of single hierarchical cubelike PbS submicrometer particles consisting of truncated octahedrons (a), cuboctahedrons (b) and cubes (c) obtained at 100 °C using 57 mg (a), 76 mg (b), and 200 mg (c) of Tu. For each case, crystals viewed down on the ⟨100⟩ directions were shown in upper rows, while those viewed from tilted directions were present in lower rows. The reaction time was listed at the bottom for each column (scale bar = 100 nm).

The pumping of $Pb(Ac)_2{\cdot}3H_2O$ solutions was finished after 6 min. The concave areas of the branched particles were gradually filled, and only slight enlargement of particle size could be observed. That is to say, there are two different growth states divided by stopping pumping $Pb(Ac)_2{\cdot}3H_2O$ solution, which is also marked by the red line in Figures 2 and 3.With reaction proceeding, such as between 8 and 15 min, some facets were developed at the corners, while those interior parts remained unshaped. The interior rough surfaces could be filled by nutrient and became smooth faces or fused together in later growth processes (after 15 min). Therefore, the branching growth in the early stage was ceased after stopping the pumping, and the faceting growth took control in the following growth processes. The time-dependent products were also characterized by transmission electron microscopy (TEM). At lower magnifications, as shown in Figure 3a−c, the geometrical contours of these samples are consistent with those observed under FESEM. The nonuniform contrast within each particle could be deduced from their morphologies. The high-resolution (HR) TEM images taken from one corner of an individual particle in both [100] and [211] zone-axes, together with their corresponding electron diffraction (ED) patterns (Figure 3d−g), confirm the highly crystalline nature of these intermediate products (here only product prepared using 76 mg of Tu at 100 °C with reaction time of 5 min was taken and used as an example). The interplanar distance of 0.30 nm corresponds to the {100} face, while 0.22 and 0.34 nm correspond to the {111} and {110} faces of the products. Insets in (d) and (f) are their corresponding fast Fourier transform transformation patterns, which are in good agreement with the ED patterns shown in (e) and (g).

The first sample for each case was obtained by interrupting the pumping of $Pb(Ac)_2{\cdot}3H_2O$ solution at 3 min. In our experiment, the nucleation should occur already before the interruption and the nuclei could grow slightly during this early stage. With the low concentration and slow addition of $Pb(Ac)_2{\cdot}3H_2O$ solution, an instantaneous nucleation was believed to occur in our processes. The continuous addition of $Pb(Ac)_2{\cdot}3H_2O$ solution caused the branching growth of these nuclei as evidenced in the first two columns in Figure 2. The branching growth could not be sustained any longer once the pumping was stopped. The growth habit of each branch on all cubelike particles was then controlled by other factors. As shown in Figure 2a, the growth of the subunits in sample was favored by an octahedral growth habit. Such growth habit was changed to cube favorable for sample in Figure 2c, and the intermediate sample in Figure 2b took the compromised habit between them. In our previous work, we found that the growth habit of PbS submicrometer particles was determined by the mole ratio of Tu to $Pb(AC)_2$ (hereafter abbreviated as $R_{S/Pb}$).[27] A lower $R_{S/Pb}$ favors octahedral growth habit, while higher $R_{S/Pb}$ is beneficial for cube growth. In the early stage after nucleation depicted in Figure 2, the growth for all particles was favored by cubic habit since there were abundant Tu in the reaction flasks. When there is not enough nutrient for branching growth, for example, after 6 min of pumping the $Pb(Ac)_2{\cdot}3H_2O$ solution,

dx.doi.org/10.1021/ic501368y | Inorg. Chem. 2014, 53, 11484−11491

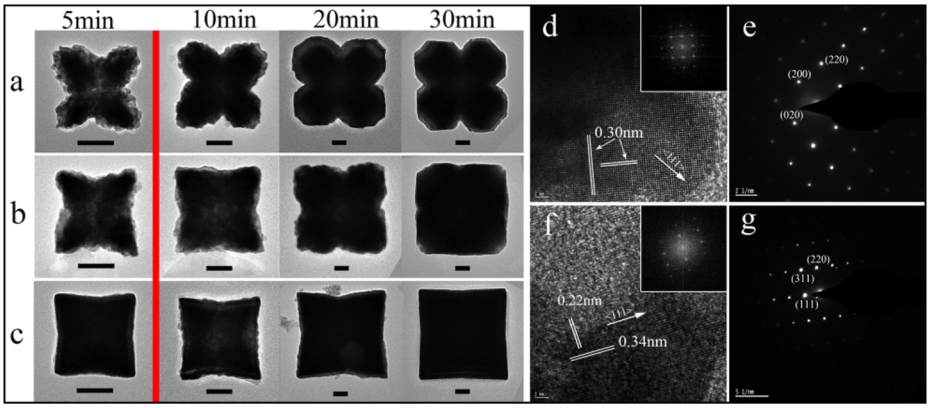

Figure 3. Time-dependent TEM images of single branched cubelike PbS submicrometer particles consisting of truncated octahedrons (a), cuboctahedrons (b), and cubes (c) obtained at 100 °C using 57 mg (a), 76 mg (b), and 200 mg (c) of Tu. The reaction time was listed at the top for each column (scale bar = 100 nm); HRTEM images (d and f) and electron diffraction patterns(e and g) of product prepared using 76 mg of Tu at 100 °C with reaction time of 5 min displayed in Figure 2b.

the growth habit was switched to be under the control of $R_{S/Pb}$. For the three reaction systems, the overall $R_{S/Pb}$ was increased from 3.7 to 13.1, and the eight small subunits constituting the three typical products consequently evolved from truncated octahedrons to cuboctahedrons and cubes.

Effect of $R_{S/Pb}$ Value on Morphology. The $R_{S/Pb}$ was further tuned via three ways to study its effects on the morphologies of PbS particles. First, we varied the amount of Tu added into the flask or the volume of $Pb(Ac)_2{\cdot}3H_2O$ solution to be pumped to change $R_{S/Pb}$. Second, we increased the reaction temperature to allow a higher decomposition rate of Tu that leads to higher $R_{S/Pb}$. Finally the chemical to be pumped was changed.

When the amount of Tu was reduced to 46 mg or the pumped volume of $Pb(Ac)_2{\cdot}3H_2O$ solution was increased to 2.0 mL, 2.5 or 3.0 mL, the corresponding total amounts of $Pb(Ac)_2{\cdot}3H_2O$ were 152, 200, and 232 mg, respectively, and the $R_{S/Pb}$ values were 1.9, 1.5, and 1.2, accordingly, while keeping the other conditions same to those for preparing PbS particles in Figure 1. When the value of $R_{S/Pb}$ was 3.0, the overall shape of the resultant product appeared to be octahedral with partially unfilled vertexes (Figure 4a). This morphology is similar to those highly grown particles in Figure 1a. The calculated value of $R_{S/Pb}$ in Figure 1a is 3.7, which is slightly higher than that used in Figure 4a. The morphological transformation from cubic to octahedral growth habit was not significant. When $R_{S/Pb}$ was reduced to 1.9, concave octahedral product was yielded as shown in Figure 4b. This result clearly manifests that lower $R_{S/Pb}$ favors the octahedral growth habit. Figure 4c shows that a mixture of hexapod-like particles and unfilled octahedral particles was produced with $R_{S/Pb}$ = 1.5. The hexapod-like structure became more prominent with the decrease of $R_{S/Pb}$ to 1.2 as shown in Figure 4d. In addition, with the increase of the volume of $Pb(Ac)_2{\cdot}3H_2O$ solution to be pumped, the driving force could be maintained at a higher level for longer time in the reaction system and caused more branching[28] as shown in Figure 4b–d.

The decomposition of Tu would be accelerated at higher temperature. To further investigate the $R_{S/Pb}$ effect on the morphologies of PbS particles, a series of reactions were performed at a higher temperature (120 °C) with increased $R_{S/Pb}$ from 1.5 to 5.0. When 57 mg of Tu was used, the resultant product was mainly comprised of cubic particles. Compared with the product obtained at 100 °C (Figure 1a)

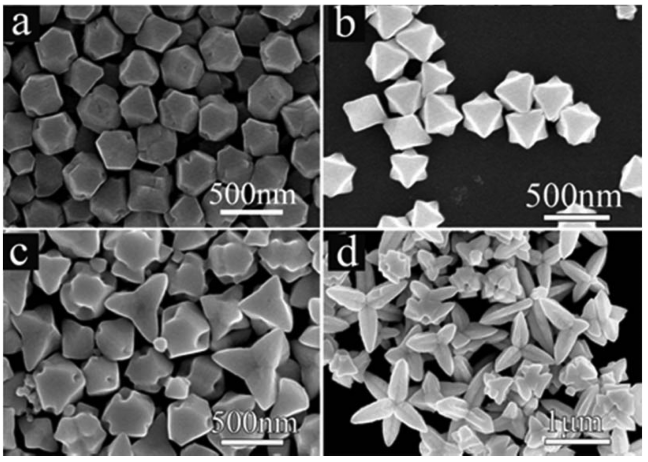

Figure 4. FESEM images of products obtained at 100 °C after 30 min reaction with different $R_{S/Pb}$: (a), $R_{S/Pb}$ = 3.0 using 46 mg of Tu and 1.0 mL of $Pb(Ac)_2{\cdot}3H_2O$ solution. (b), $R_{S/Pb}$ = 1.9 using 57 mg of Tu and 2.0 mL of $Pb(Ac)_2{\cdot}3H_2O$ solution. (c), $R_{S/Pb}$ = 1.5 using 57 mg of Tu and 2.5 mL of $Pb(Ac)_2{\cdot}3H_2O$ solution. (d), $R_{S/Pb}$ = 1.2 using 57 mg of Tu and 3.0 mL of $Pb(Ac)_2{\cdot}3H_2O$ solution. The concentration of $Pb(Ac)_2{\cdot}3H_2O$ solution and other conditions were same to those used in Figure 1.

with same $R_{S/Pb}$ of 3.7, the hierarchical structure disappeared (Figure 5a and Supporting Information, Figure S5). In addition, the size distribution became broader suggesting a progressive nucleation might also occur along with a shrink of particle size. The average size is ~350 nm. Similar phenomenon could be observed for the case when 68 ($R_{S/Pb}$ =4.5, Supporting Information, Figure S6) or 76 mg of Tu ($R_{S/Pb}$ = 5.0, Figure 5b and Supporting Information, Figure S7) was added into the reaction flask. Cubelike particles consisting of eight cuboctahedral subunits became cubic particles with average particle sizes less than 500 nm. Meanwhile, when the volume of $Pb(Ac)_2{\cdot}3H_2O$ solution was doubled (Figure 5c), the $R_{S/Pb}$ value was halved from 3.7, and a similar morphology to the highly grown particles in Figure 1a appeared. Further decreasing the $R_{S/Pb}$ to 1.5 by using 46 mg of Tu and doubled volume of $Pb(Ac)_2{\cdot}3H_2O$ solution (Figure 5d), the particles have similar hierarchical structure to those dominant product in Figure 1a.

When $Pb(Ac)_2{\cdot}3H_2O$ solution was added into the flask and Tu solution was pumped into the reaction system, the growth

dx.doi.org/10.1021/ic501368y | Inorg. Chem. 2014, 53, 11484–11491

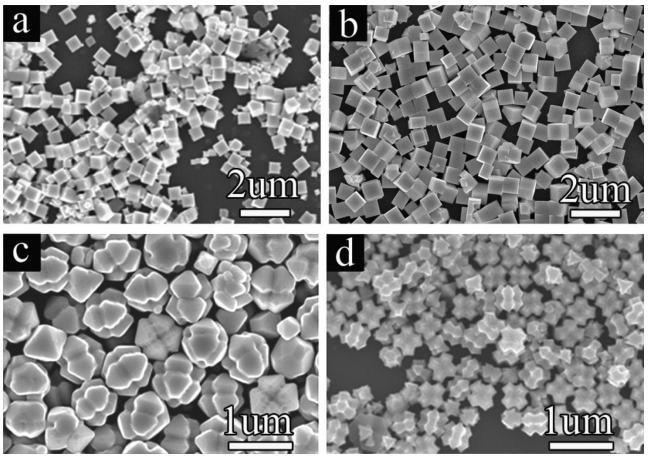

Figure 5. FESEM images of the products obtained at 120 °C after 30 min reactions with $R_{S/Pb}$ values of 3.7 (a), 5.0 (b), 1.9 (c), and 1.5 (d). The weight of Tu dissolved in the flask, the volume of $Pb(Ac)_2{\cdot}3H_2O$ EG solution pumped and the weight of $Pb(Ac)_2{\cdot}3H_2O$ contained in it are (a): 57 mg of Tu + 1.0 mL of EG containing 76 mg of $Pb(Ac)_2{\cdot}3H_2O$, (b): 76 mg of Tu + 1.0 mL of EG containing 76 mg of $Pb(Ac)_2{\cdot}3H_2O$, (c): 57 mg Tu +2.0 mL of EG containing 152 mg of $Pb(Ac)_2{\cdot}3H_2O$, (d): 46 mg of Tu + 152 mg of $Pb(Ac)_2{\cdot}3H_2O$ dissolved in 2.0 mL of EG.

habit changed as well. In Figure 6a, the experimental condition is almost identical to that used in Figure 1a except exchanging

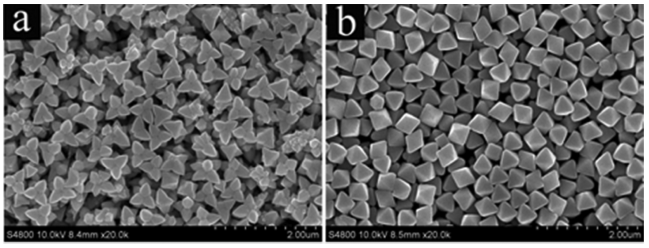

Figure 6. FESEM images of the products prepared using different pumping manner. (a) 1.0 mL of Tu/EG solution containing 57 mg of Tu pumped into 8.0 mL of $Pb(Ac)_2{\cdot}3H_2O$ EG solution containing 76 mg of $Pb(Ac)_2{\cdot}3H_2O$, the other conditions were same to those in Figure 1a; (b) the experimental conditions were same to (a) except increasing the reaction temperature to 120 °C.

the chemicals in the flask or to be pumped. Similar change also occurs for Figure 6b and 5b. For both cases, the octahedral growth habit instead of cubic growth habit (Figure 1a and 5b) played a dominant role here. Branching octahedral and nearly perfect octahedral particles were obtained for reactions carried out at 100 and 120 °C, respectively. Once the pumping of either Tu or $Pb(Ac)_2{\cdot}3H_2O$ solution is finished, the reaction conditions for two reactions with reversed addition of chemicals were similar. Their different growth habit could be attributed to the nucleation or growth process during the early stage.

DISCUSSION

On the basis of the above observations, the formation of hierarchical structure of PbS micrometer particles can be deduced as follows and explained by the theorems of Berg and Sunagawa. First, cubelike nuclei were formed at high $R_{S/Pb}$ favorite cube growth habit during the nucleation stage. Then, the branches grew out from the nuclei due to diffusion-dominated growth under high concentration of growth unit, which were achieved by the continuous pumping of $Pb(Ac)_2{\cdot}3H_2O$ solution. In such situation, the growth rate was faster than the diffusion rate, and the corners most closed to the inner solution would grow fast to form the branches.[29] This is consistent with the well-known Berg effect. Similar diffusion-dominated growths were also applied in forming concave palladium nanocubes and hopper PbTe structure.[30,31] Sunagawa correlated the growth mechanism with driving force, that is, the concentration of the growth unit. The driving force has two critical values.[28] When it exceeds the higher critical values, an adhesive-type growth mechanism, which is also referred to as branching growth, will be adopted, and the final products usually take dendrite morphology. When it is less than the lower one, the growth will be principally controlled by spiral growth mechanisms. In between these two values, two-dimensional growth (layer-by-layer) occurs. In our cases, after finishing the pumping, the driving force in the system would drop significantly, and further growth was mainly controlled by the spiral growth mechanism. After branching, there were many kinks or/and steps having high affinity toward growth unit on the branches as well as within the gaps among the branches. The following formations of flat facets first on the cusps, filling the gaps, and fusing of neighboring small polyhedral particles, all took place in these active sites via surface diffusion of growth units. Finally each branch gradually developed into a polyhedron, which fused with neighboring others to form a hierarchical particle.

It was noticed that all the products shown in Figure 1 presented good monodispersity. In our synthesis, both the concentration of reactants and reaction temperature were kept at low levels to allow slow reactions between the two chemicals. The continuous pumping of $Pb(Ac)_2{\cdot}3H_2O$ solution could build up the concentration of PbS growing unit progressively before the commencement of nucleation. The slow buildup concentration of growth unit, along with the low concentration of reactants in the system, made the instantaneous nucleation process possible and hindered the progressive nucleation. Therefore, the control of particle size could be achieved as we showed in above experimental results.

At the early stages of the growth processes, all the branches unanimously extended to the eight ⟨111⟩ directions, which should be the result of cube-favorite growth habit and diffusion-dominated growth, while at the late stages, that is, after finishing the pumping, growth rate slowed down and became decisive for the crystal growth. The growth rate difference among the different planes distinguished and exerted its influence to the morphologies of the products. Just as we discussed earlier, the different values of $R_{S/Pb}$ led to the subunits of the hierarchical structure having different shapes, such as truncated octahedrons, cuboctahedrons, and cubes.

Though we have known the formation mechanism of the products and the influence factors to the morphologies, there are still two experimental phenomena that might be confusing. First, comparing the products shown in Figure 1a,b with those shown in Figure 1d,e, it was found that the hierarchical structures turned more inconspicuous with increased concentration of Tu. That is to say, branching growth happened more easily at low concentration of growth unit. This observation does not conform to general knowledge that branching growth should occur at high concentration of growth unit due to diffusion-rate controlled growth. Second, comparing the products shown in Figure 2a−c, the particle with more

dx.doi.org/10.1021/ic501368y | Inorg. Chem. 2014, 53, 11484−11491

obviously branched corners grown under high concentration of Tu turned more inconspicuous as the growth proceeds, while the particle grown under low concentration of Tu became more branched.

To explain these observations, understandings of both the nucleation and growth processes are required. Although some in situ observations on the nucleation and particle growth of noble metallic and semiconductor nanocrystals have been achieved recently,[32,33] it is still a challenge for current instruments to precisely determine the nucleation and growth rates based on quantitative investigation due to the short time scale of nucleation and many hidden uncertainties for these two processes. A qualitative analysis based on tradition nucleation and growth theories may help us to understand the formation mechanisms of PbS particles in our process.

In the classical nucleation theory, the nucleation rate could be expressed as[34]

$$J = A \exp\left[\frac{16\pi\gamma^3 V^2}{3k^3T^3(\ln S)^2}\right] \quad (1)$$

Here, J is the number of nuclei formed per unit time per unit volume, A is the nucleation constant, γ is the interfacial tension between the surface of nuclei and the supersaturation solution, V is the volume of growth unit, k is the Boltzmann constant, T is the temperature, and S is the supersaturation degree.

In growing single crystals from solutions, Sunagawa correlated the growth rate of a specific facet with driving force,[28] which is determined by the supersaturation degree of the growth unit and could be expressed as

$$S = \frac{C_\infty}{C} \quad (2)$$

$$\frac{\Delta\mu}{kT} = \ln S \quad (3)$$

Here $\Delta\mu$, C_∞, and C are, respectively, the difference of the chemical potentials between the saturated solution and the solid phase, concentrations of growth unit in the bulk solution and on the surface of the growing facet. S, k, and T have their normal meanings as shown above. $\Delta\mu/kT$ is the driving force.

From the equations mentioned above, it can be deduced that both the nucleation and growth processes are related to S. However, the S presented in eq 1 is not the same one as that in eqs 2 and 3 though they have the same normal meaning as supersaturation degree, for they represented different stages during the formation of crystals. The homogeneous nucleation process is instantaneous and hardly captured. At the moment of nucleation, the value of S is special and cannot be changed any more. By comparison, the growth process is long and easily observed as we have done in Figure 2. The value of S is changeable and can be adjusted such as by pumping the reactants. Besides, the driving force for a single crystal nucleus to grow during the growth process should be decided by the supesaturation degree around each individual nucleus not that for the whole reaction system, so here we introduced local supesaturation degree (LSD) to describe the microenvironment of an individual nucleus for crystal growth. Then, the expression of S in eq 3 should be modified as LSD. Obviously, LSD is related to the supersaturation degree for the whole reaction system and the number of the crystal nuclei (N) in the reaction solution.

For the PbS particles prepared in our system, the increased amount of Tu predissolved in the flask only means the increased supersaturation during the nucleation stage instead of during the whole growth process, while branching growth occurs in the growth process. So the branch degree of the final products does not have direct consequence with the amount of Tu predissolved in the flask.

During the nucleation stage, the number of nuclei (N) is approximately to be the product of J times the volume of the reaction solution. For a homogeneous nucleation process, J would increase rapidly with increasing S if the critical value of supersaturation was exceeded.[29] For the synthesis shown in Figures 1 and 2, the only variable is the amount of Tu added into the flask. In addition, compared with the amount of $Pb(Ac)_2{\cdot}3H_2O$ solution pumped to the reaction system before nucleation started, the amount of Tu is far in excess, and the introduction time of nucleation for each reaction should be comparable as it is determined from the amount of $Pb(Ac)_2{\cdot}3H_2O$ solution pumped. Assuming the critical value of supersaturation during the instantaneous nucleation process was constant, N would be determined by the weight of Tu added, or in other words the sulfur specie decomposed from Tu. According to eq 1, fewer nuclei (also the number of particles evolved from them) would be formed for the case using 57 mg of Tu than the other cases using more Tu. As a result, the LSD during the growth stage for the case using 57 mg of Tu might be larger than the other cases for the same amount of $Pb(Ac)_2{\cdot}3H_2O$ solution was pumped into the reaction system. The LSD should be a compromise between N and C_∞ and a larger C_∞ before the nucleation process cannot guarantee a higher LSD. On the other hand, for the case using 57 mg of Tu, there should be more growth units for each individual particle to grow than other cases due to less N since the total growth units are same in all the cases shown in Figure 1, which means more growth units are available to fill the gaps among branched polyhedral subunits and increase their fusion degree. So large LSD might result in more growth units for individual particle, and the former unit favors the branch growth, while the latter unit favors the fusion growth. The two contrary factors exert their influence on the morphologies of the products simultaneously. If the effect of LSD takes control of product morphology, larger LSD would favor the products with much obvious hierarchical structure as shown in Figure 1a,b,d,e; if the effect of the amount of growth units plays a decisive role, more growth units would led to inconspicuous hierarchical structure as shown in Figure 1b−d.

For reactions carried out at 120 °C, the decomposition of Tu was favored, and reaction temperature was a plus for increasing N according to eq 1 (Figure 5, Figure 6b, and Supporting Information, Figures S5−S7). This increase in N is fairly significant and causes the LSDs to drop rapidly shortly after nucleation processes. Supporting Information, Figures S5−S7 give the time-dependent FESEM images of the products obtained under the same reaction conditions as those in Figure 1a−c, respectively, except reaction temperature. Their morphologies differ from those shown in Figures 1 and 2, where massive kinks and steps were produced due to the branching growth. It was only in the early stage (3 min) that the products appeared slightly branched. A spiral growth mechanism might be dominant, and the two-dimensional growth could be unlikely attained since the LSDs were low. So larger N and relatively lower LSD led to the formation of cubelike particles with less branching (Supporting Information,

dx.doi.org/10.1021/ic501368y | Inorg. Chem. 2014, 53, 11484−11491

Figures S5−S7). Similar suppression of branching was also observed in the case of preparing octahedral particles in Figure 6b.

Let us come to the second conclusion. The particles prepared using 200 mg of Tu appeared to have more obviously branched corners than the others at the early stage of the growth process, which reflected that the LSD in such case was highest for there were maximum of Tu. With the growth proceeding and the particles growing larger, the large amount of particles led to the rapid consumption of the growth unit, and the LSD declined more quickly than it did in other cases and turned out to be the smallest to form most inconspicuous hierarchical structure.

CONCLUSIONS

In summary, the morphological evolutions of submicrometer PbS particles from small cubes to hierarchical cubelike ones consisting of eight polyhedral subunits and to cubes again have been demonstrated in solution processes. The formation of these particles was synergistically controlled by the growth habit and LSD of PbS particles. The cubic growth habit was favored at high $R_{S/Pb}$. The synthesis of hierarchical cubelike particles consisting of different polyhedral subunits could be delimited into two stages separated by the draining of the $Pb(Ac)_2{\cdot}3H_2O$ solution. Branching of these cubelike particles could be attained at comparatively higher LSDs with continuous pumping of reactant, while faceting growth took place at later stage of growth process after finishing pumping $Pb(Ac)_2{\cdot}3H_2O$ solution. As a compromise between the number of nuclei and bulk concentration, relatively higher LSD of the growing particle might be achieved at less overall concentration of reactant and lower temperature because there are fewer nuclei formed during the nucleation process. This concept could explain the different fusion degrees of hierarchical cubelike particles consisting of cuboctahedral subunits and less branching growth for particles obtained at 120 °C. Our findings might be used to interpret the formation mechanism of submicrometer particles.

ASSOCIATED CONTENT

Supporting Information

Patterns of XRD and FESEM images. This material is available free of charge via the Internet at http://pubs.acs.org.

AUTHOR INFORMATION

Corresponding Authors

*E-mail: chenfa@cec.sc.edu. (F.-L.C.)
*E-mail: cwang@ciac.jl.cn. (C.W.)

Present Address

[⊥]Department of Materials Science and Engineering, National University of Singapore, Blk E3A #03−14, 7 Engineering Drive 1, Singapore 117574.

Author Contributions

The manuscript was written through contributions of all authors. All authors have given approval to the final version of the manuscript.

Author Contributions

[‖]These authors contributed equally.

Notes

The authors declare no competing financial interest.

ACKNOWLEDGMENTS

The authors are grateful for the financial support from National Natural Science Foundation of China (NSFC) through the Major Research Plan (91022005), NSFC (21171159), and the Innovative Research Groups (21221061), Fanglin Chen is supported by the HeteroFoaM Center, an Energy Frontier Research Center funded by the U.S. Department of Energy (DOE), Office of Science, Basic Energy Sciences (BESs), under Award No. DE-SC0001061.

REFERENCES

(1) Zhou, Z.-Y.; Tian, N.; Li, J.-T.; Broadwell, I.; Sun, S.-G. *Chem. Soc. Rev.* **2011**, *40*, 4167−4185.
(2) Sun, Y.; Xia, Y. *Science* **2002**, *298*, 2176−2179.
(3) Bratlie, K. M.; Lee, H.; Komvopoulos, K.; Yang, P.; So-morjai, G. A. *Nano Lett.* **2007**, *7*, 3097−3101.
(4) Zhang, D.-F.; Zhang, H.; Guo, L.; Zheng, K.; Han, X.-D.; Zhang, Z. *J. Mater. Chem.* **2009**, *19*, 5220−5225.
(5) Kruszynska, M.; Borchert, H.; Parisi, J.; Kolny-Olesiak, J. *J. Am. Chem. Soc.* **2010**, *132*, 15976−15986.
(6) LaMer, V. K.; Dinegar, R. H. *J. Am. Chem. Soc.* **1950**, *72*, 4847−4854.
(7) Wagner, R. S.; Ellis, W. C. *Appl. Phys. Lett.* **1964**, *4*, 89−90.
(8) Duan, X.; Lieber, C. M. *Adv. Mater.* **2000**, *12*, 298−302.
(9) Morin, S. A.; Bierman, M. J.; Tong, J.; Jin, S. *Science* **2010**, *328*, 476−480.
(10) Buckley, H. E. *Crystal Growth;* Wiley: New York, 1951.
(11) Zhou, G. J.; Lu, M. K.; Xiu, Z. L.; Wang, S. F.; Zhang, H. P.; Zhou, Y. Y.; Wang, S. M. *J. Phys. Chem. B* **2006**, *110*, 6543−6548.
(12) Wang, Y.; He, J.; Liu, C.; Chong, W. H.; Chen, H. *Angew. Chem., Int. Ed.* **2014**, DOI: 10.1002/anie.201402986.
(13) Wang, Q.; Chen, G.; Yin, H. *J. Mater. Chem. A* **2013**, *1*, 15355−15369.
(14) Wulff, G.; Zeitschrift, F. *Krystallogr.* **1901**, *34*, 449−530.
(15) Siegfried, M. J.; Choi, K.-S. *Angew. Chem., Int. Ed.* **2008**, *47*, 368−372.
(16) Siegfried, M. J.; Choi, K.-S. *Angew. Chem., Int. Ed.* **2005**, *44*, 3218−3223.
(17) Siegfried, M. J.; Choi, K.-S. *J. Am. Chem. Soc.* **2006**, *128*, 10356−10357.
(18) Machol, J. L.; Wise, F. W.; Patel, R. C.; Tanner, D. B. *Phys. Rev. B* **1993**, *48*, 2819−2822.
(19) Nair, P. K.; Gomezdaza, O.; Nair, M. T. S. *Adv. Mater. Opt. Electron.* **1992**, *1*, 139−145.
(20) Lee, H.; Leventis, H. C.; Moon, S.-J.; Chen, P.; Ito, S.; Haque, S. A.; Torres, T.; Nüesch, F.; Geiger, T.; Zakeeruddin, S. M.; Grätzel, M.; Nazeeruddin, M. K. *Adv. Funct. Mater.* **2009**, *19*, 2735−2742.
(21) H. Sargent, E. *Adv. Mater.* **2005**, *17*, 515−522.
(22) Lee, S.-M.; Jun, Y.-w.; Cho, S.-N.; Cheon, J. *J. Am. Chem. Soc.* **2002**, *124*, 11244−11245.
(23) Bierman, M. J.; Lau, Y. K. A.; Kvit, A. V.; Schmitt, A. L.; Jin, S. *Science* **2008**, *320*, 1060−1063.
(24) Fan, D.; Thomas, P. J.; O'Brien, P. *J. Am. Chem. Soc.* **2008**, *130*, 10892−10894.
(25) Schliehe, C.; Juarez, B. H.; Pelletier, M.; Jander, S.; Greshnykh, D.; Nagel, M.; Meyer, A.; Foerster, S.; Kornowski, A.; Klinke, C.; Weller, H. *Science* **2010**, *329*, 550−553.
(26) Bierman, M. J.; Albert Lau, Y. K.; Jin, S. *Nano Lett.* **2007**, *7*, 2907−2912.
(27) Peng, Z.; Jiang, Y.; Song, Y.; Wang, C.; Zhang, H. *Chem. Mater.* **2008**, *20*, 3153−3162.
(28) Sunagawa, I. *Crystals: Growth, Morphology, and Perfection;* Cambridge University Press: Cambridge, U.K., 2005.
(29) Berg, W. F. *Proc. R. Soc. London, Ser. A* **1938**, *164*, 79−95.
(30) Jin, M.; Zhang, H.; Xie, Z.; Xia, Y. *Angew. Chem., Int. Ed.* **2011**, *50*, 7850−7854.

(31) Zhu, T.-J.; Chen, X.; Cao, Y.-Q.; Zhao, X.-B. *J. Phys. Chem. C* **2009**, *113*, 8085−8091.
(32) Zheng, H.; Smith, R. K.; Jun, Y.-w.; Kisielowski, C.; Dahmen, U.; Alivisatos, A. P. *Science* **2009**, *324*, 1309−1312.
(33) Langille, M. R.; Zhang, J.; Personick, M. L.; Li, S.; Mirkin, C. A. *Science* **2012**, *337*, 954−957.
(34) Mullin, J. W. *Crystallization;* Butterworth-Heinemann: Oxford, U.K., 2001.